

PAPER • OPEN ACCESS

# The dependence of confinement on the isotope mass in the core and the edge of AUG and JET-ILW H-mode plasmas













To cite this article: P.A. Schneider *et al* 2022 *Nucl. Fusion* **62** 026014

View the [article online](#) for updates and enhancements.

You may also like

- [Suppression of toroidal Alfvén eigenmodes by the electron cyclotron current drive in KSTAR plasmas](#)  
J. Kim, J. Kang, T. Rhee et al.
- [Orbit tomography of energetic particle distribution functions](#)  
L. Stagner, W.W. Heidbrink, M. Salewski et al.
- [Prediction of divertor heat flux width for ITER pre-fusion power operation using BOUT++ transport code](#)  
X.X. He, X.Q. Xu, Z.Y. Li et al.

# The dependence of confinement on the isotope mass in the core and the edge of AUG and JET-ILW H-mode plasmas

P.A. Schneider<sup>1,\*</sup> , C. Angioni<sup>1</sup> , L. Frassinetti<sup>2</sup> , L. Horvath<sup>3</sup> , M. Maslov<sup>3</sup>, F. Auremma<sup>4</sup> , M. Cavedon<sup>1,5</sup>, C.D. Challis<sup>3</sup>, E. Delabie<sup>6</sup>, M.G. Dunne<sup>1</sup>, J.M. Fontdecaba<sup>7</sup> , J. Hobirk<sup>1</sup> , A. Kappatou<sup>1</sup> , D.L. Keeling<sup>3</sup>, B. Kurzan<sup>1</sup>, M. Lennholm<sup>3</sup>, B. Lomanowski<sup>6</sup>, C.F. Maggi<sup>3</sup> , R.M. McDermott<sup>1</sup> , T. Pütterich<sup>1</sup> , A. Thorman<sup>3</sup>, M. Willensdorfer<sup>1</sup> , the ASDEX Upgrade Team<sup>a</sup>, the EUROfusion MST1 Team<sup>b</sup> and JET Contributors<sup>c</sup>

<sup>1</sup> Max-Planck-Institut für Plasmaphysik, Boltzmannstr. 2, 85 748 Garching, Germany

<sup>2</sup> KTH Royal Institute of Technology, Teknikringen 31, Sweden

<sup>3</sup> United Kingdom Atomic Energy Authority, Culham Centre for Fusion Energy, Culham Science Centre, Abingdon, Oxon, OX14 3DB, United Kingdom

<sup>4</sup> Consorzio RFX-CNR, ENEA, INFN, Università di Padova, Acciaierie Venete SpA, Padova, Italy, CNR-ISTP, Corso Stati Uniti 4, 35 127 Padova, Italy

<sup>5</sup> Dipartimento di Fisica ‘G. Occhialini’, Università di Milano-Bicocca, Milano, Italy

<sup>6</sup> Oak Ridge National Laboratory, Oak Ridge, TN 37 831, United States of America

<sup>7</sup> Laboratorio Nacional de Fusión Ciemat, E-28040 Madrid, Spain

E-mail: [philip.schneider@ipp.mpg.de](mailto:philip.schneider@ipp.mpg.de)

Received 31 May 2021, revised 26 October 2021

Accepted for publication 30 November 2021

Published 22 December 2021



## Abstract

Experiments in ASDEX Upgrade (AUG) and JET with the ITER-like wall (JET-ILW) are performed to separate the pedestal and core contributions to confinement in H-modes with different main ion masses. A strong isotope mass dependence in the pedestal is found which is enhanced at high gas puffing. This is because the ELM type changes when going from D to H for matched engineering parameters, which is likely due to differences in the inter ELM transport with isotope mass. The pedestal can be matched in H and D plasmas by varying only the triangularity and keeping the engineering parameters relevant for core transport the same. With matched pedestals Astra/TGLF (Sat1geo) core transport simulations predict the experimental profiles equally well for H and D. These core transport simulations show a negligible mass dependence and no gyro-Bohm scaling is observed. However, to match the experimental observations at medium  $\beta$  it is required to take the fast-ion dilution and rotation

\* Author to whom any correspondence should be addressed.

<sup>a</sup> See Meyer *et al* 2019 (<https://doi.org/10.1088/1741-4326/ab18b8>) for the ASDEX Upgrade Team.

<sup>b</sup> See Labit *et al* 2019 (<https://doi.org/10.1088/1741-4326/ab2211>) for the EUROfusion MST1 Team.

<sup>c</sup> See Joffrin *et al* 2019 (<https://doi.org/10.1088/1741-4326/ab2276>) for the JET Contributors.



Original content from this work may be used under the terms of the [Creative Commons Attribution 4.0 licence](https://creativecommons.org/licenses/by/4.0/). Any further distribution of this work must maintain attribution to the author(s) and the title of the work, journal citation and DOI.

into account. This is not enough for high  $\beta$  plasmas where for the first time a profile match between H and D plasmas was achieved experimentally. Under these conditions quasilinear modelling with TGLF over predicts the transport in the core of H and D plasmas alike.

Keywords: tokamak, heat transport, isotope effect, pedestal stability, quasilinear modelling

(Some figures may appear in colour only in the online journal)

## 1. Introduction

The isotope mass dependence of confinement is a long standing open question in tokamak physics. In multi-machine studies the global confinement time is found to scale with  $M^{0.2}$  where  $M$  is the main ion mass number [1]. However, this global number incorporates edge and core physics at the same time while we know that they can scale differently [2].

The plasma edge or the pedestal shows a strong dependence on the main ion mass in AUG [3–5] as well as in JET-ILW [6, 7], most notably the pedestal density is lower in H for matched engineering parameters—like power, gas, plasma shape—while the temperatures can be similar resulting in lower pressure. Three main factors which set the pedestal top are important to consider, to understand the origin of this difference: ELM stability, ELM losses and inter ELM transport.

ELM stability is the main candidate. In principle, a mass dependence could be introduced via diamagnetic stabilisation [8, 9], however, this effect was found to be small for the JET-ILW pulses discussed here [7]. Profile parameters which change between H and D can have an impact on the ELM stability. A shift of the density profile or an increasing separatrix density lowers the pedestal pressure at which ELMs are triggered [10, 11]. Also an increase of the separatrix temperature due to changes in the divertor condition can have an influence on the ELM stability [7]. Both mechanisms will be discussed in this paper.

ELM losses  $P_{\text{loss,ELM}}$  were found to have an impact on the pedestal top in D plasmas [12]. Since the ELM behaviour is different in H and D plasmas, with typically higher frequencies in H, this was tested in AUG [3] and JET-ILW [7]. However, since the ELM frequency is strongly correlated to the ELM size,  $P_{\text{loss,ELM}}$  is not varying enough between isotopes to be sufficient to explain the observed differences in the pedestal. This is why we assume the impact of the ELM losses to be negligible.

The inter ELM transport, is the least understood part of the three candidates to explain the isotope dependence in the pedestal. The theoretical understanding of the heat and particle transport in the H-mode pedestal is an active field of research, however, due to the steep gradients reliable simulations are difficult, but can be expected in the upcoming years. For L-mode plasmas drift waves were found in the edge and show properties explaining the observed mass dependence of transport [13, 14] and it is possible that collisional drift waves also play

an important role in H-mode. While interpretative experimental studies regularly find that the transport in H is larger than in D [7, 15], the uncertainties in these studies are substantial. In particular, due to the mass dependence in the pedestal a trade off between matching the sources or matching the profiles has to be made. Due to the lack of theoretical understanding of the pedestal physics it is difficult to distinguish a source related impact (profile stiffness, electron-ion equipartition) or changing profiles (collisionality,  $T_i/T_e$ , etc) from the actual impact the ion mass has.

Very similar to the plasma edge different factors influence the core transport. The main ion mass is expected to be one of these factors. The scaling of mass and transport is also not constant and can vary depending on the plasma regime. Non-linear gyrokinetic simulations provide the foundation for our theoretical understanding. For example trapped electron mode turbulence with a strong dependence on collisions [16] does scale differently than ion temperature gradient (ITG) driven turbulence with adiabatic electrons in the collisionless limit [4, 17]. However, when considering the influence of collisions [4, 13],  $E \times B$  shear [18] and  $\beta$  stabilisation physics [18] for ITG turbulence the expected scaling with main ion mass will change. A more complete account of the different physics mechanisms depending on the main ion mass can be found in [19].

In addition to the direct impact of the main ion mass on turbulent transport, there are the indirect effects due to operational constraints which become important when testing theory against the experiment. The mass dependence in the electron-ion equipartition [20] and the fast-ion slowing down [4, 21] can result in different transport properties. The same is true for the mass dependence originating from the edge—because the pedestal is strongly coupled with the plasma core [22, 23]. Then there are more trivial differences like electron and ion heat fractions and different torque which need to be taken into account.

It can be summarized that a pure gyro-Bohm scaling of the core transport with a  $M^{-0.5}$  dependence is not expected by theory. While a gyroradius dependence is the core of most gyrokinetic models, the state of the art models incorporate additional physics mechanisms which results in a more complete description of the experimentally observed phenomena.

To address the question of the heat transport dependence with the main ion mass series of plasma discharges has been conducted with highly resolved measurements in the tokamaks ASDEX Upgrade (AUG) and JET with the ITER-like wall (JET-ILW). In section 2 we give a short overview of the two

tokamaks AUG and JET-ILW and will describe the details of the experimental scans—which allows us for the first time to distinguish different contributions to the heat transport—and introduce the modelling framework applied. The results are described separately, first the impact observed on the pedestal in section 3, then we select pairs with matched pedestal for a detailed core transport analysis in section 4 and discuss the core–edge coupling for the whole data set.

## 2. Experimental and modelling setup

AUG and JET-ILW are both metal tokamaks with a tungsten divertor. In AUG also the main chamber walls are tungsten while in JET-ILW they are coated with beryllium, which is the setup foreseen for ITER. The metal wall results in a relatively low concentration of low  $Z$  impurities and consequently an effective charge  $Z_{\text{eff}}$  of typically below 1.5 in both devices. To improve ion temperature measurements small amounts of low- $Z$  impurities are introduced into the plasma externally. In JET-ILW this is neon in H and D plasmas and in AUG nitrogen in H plasmas. The main plasma parameters in AUG are a plasma current of  $I_p = 0.8$  MA and a toroidal magnetic field  $B_t = -2.5$  T with an edge safety factor of  $q_{95} = 5.2$ . In JET-ILW  $I_p = 1.4$  MA and  $B_t = 1.7$  T with  $q_{95} = 3.7$  is used with the corner–corner C/C divertor configuration which has the strike points in the inner and outer corner close to the divertor pumping location. The applied heating power is between 7–22 MW in AUG and 5–15 MW in JET-ILW. Since JET-ILW is twice the size of AUG, JET-ILW has about 2/3 lower  $\rho_*$  than AUG. The difference in size also means the power density in AUG is substantially higher than in JET-ILW for the presented discharge set, which results in higher relative fast-ion content in AUG compared to JET-ILW.

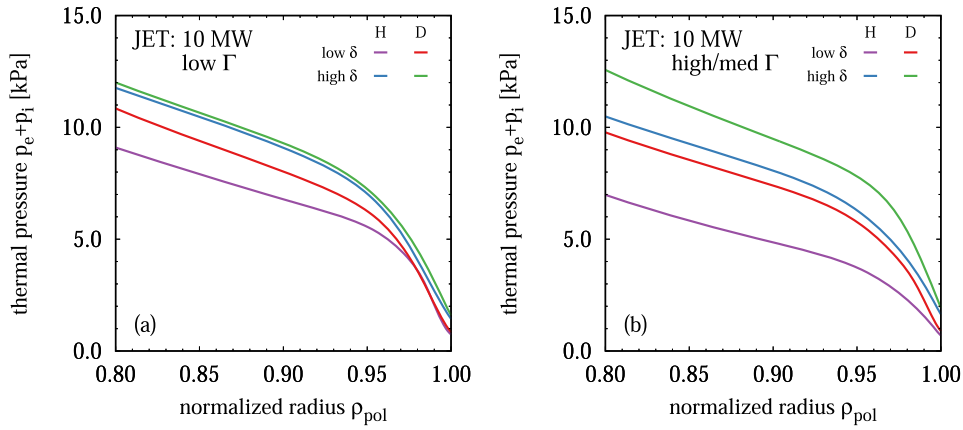
In order to overcome the limitation of the NBI in hydrogen and to achieve higher NBI heating powers, D-NBI heating is used for dominantly H and D plasmas. This decreases the isotope purity of the plasma and H concentrations of  $n_H/(n_H + n_D) \simeq 0.9$  are achieved. While not discussed in detail here, no indication was found that the residual 10% of D alters the main conclusions of this study. D plasmas in JET-ILW have 1%–2% residual H while it is up to 5% in AUG. The gas puffing rate  $\Gamma$  [24, 25] will be quoted as ‘low’ or ‘high’. A low  $\Gamma$  is in both machines close to the lowest puffing rate for which the plasmas are considered reliably stable against impurity accumulation. A high  $\Gamma$  is a multiple of the low gas puffing rate, but still in the range where a linear pedestal response to the fuelling rate is expected. It has to be noted that the gas puffing rate is an engineering parameter and does not necessarily correspond to the ionisation source profile in the plasma, which for example also depends on the wall recycling and is the relevant quantity for the particle transport. Unfortunately, no measurements of the ionisation source are available for our data set, the same is true for sophisticated modelling which might help to predict the ionisation sources for the different plasma parameters. Existing studies suggest that the ionisation source profile within the last closed flux surface increases with lower  $M$  under otherwise similar conditions [26]. If these results were applicable to the plasmas discussed in section 3 it

would enhance the observed effects. Therefore, we keep  $\Gamma$  as general proxy for the particle sources.

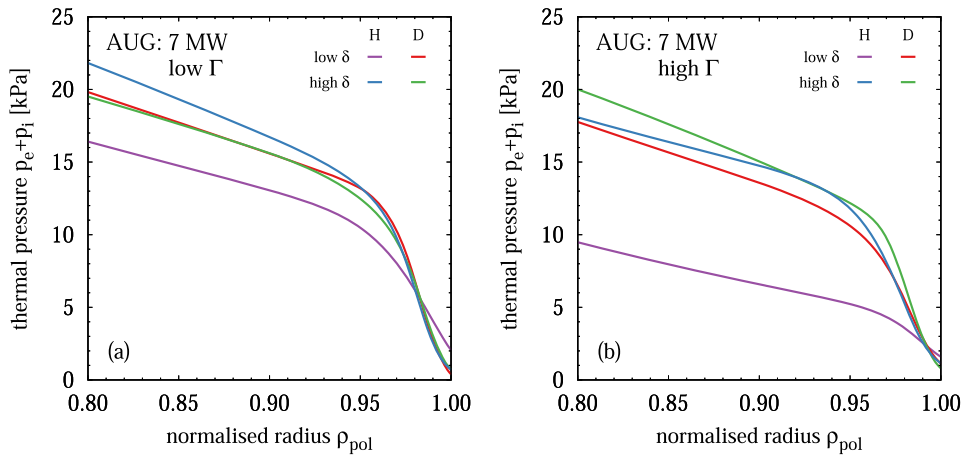
To provide a robust experimental bases for the comparison with theory, we scan the main ion mass, the heating power  $P$ , gas puffing  $\Gamma$  and plasma triangularity  $\delta$  in AUG and JET-ILW. While  $M$ ,  $P$  and  $\Gamma$  are routinely varied in similar studies, including also  $\delta$  serves a particular purpose here. As introduced in section 1 our core and edge plasma are coupled leading to an underdetermined system when only varying  $M$ ,  $P$  and  $\Gamma$ . The triangularity does break the core–edge coupling because its impact on core transport is inverse to its impact on the pedestal [27, 28]. Additionally, the impact of  $\delta$  on the core plasma is considerably lower than on the pedestal. Translating the findings at TCV [27], suggest an impact of lower than 10% for the range applied for AUG  $\delta \in [0.22, 0.37]$  and JET-ILW  $\delta \in [0.21, 0.30]$  in the core compared to 50% in the edge [28]. Considering AUG and JET-ILW are larger devices than TCV one would expect that the impact of an edge quantity like  $\delta$  [4] is further reduced in the core of AUG or JET-ILW plasmas. This is confirmed by a  $\delta$  scan performed in an AUG L-mode plasma, where no impact of the shape is found in the edge or the core of the plasma. The new strategy to vary  $\delta$  and  $M$  allows us to keep the sources the same while also matching the profiles of H and D plasma. This opens up an angle for investigation of the isotope mass dependence complementary to previous studies relying on source or profile changes.

The advantage of keeping the source profiles the same becomes apparent if we consider the different parameters involved. We expect a mass dependence of the heat flux  $Q \propto M^\mu$  with  $\mu \in [-0.5, 0.5]$  while our expected temperature dependence is  $Q \propto T^{2.5}$ . When varying the sources the temperature can change temperature change by a factor of 2, the same as a change of  $M$  from H to D. Then one compares different contributions, the one due to the mass of  $2^{0.5} = 1.4$  and the one of the temperature  $2^{2.5} = 5.7$ , consequently, a 10% uncertainty in the treatment of the temperature could mask or suggest an isotope dependence.

In our study we take temperature dependence in the heat transport into account by using the TGLF model with saturation rule Sat1geo [29] within Astra [30, 31] which allows us simulate the heat and particle transport over the whole plasma core. This means we run predictive flux driven simulations and for similar simulations using saturation rule Sat1 it was found that due to high stiffness the profiles can relax to the critical gradient [6]. This means the dependencies apart of those influencing the critical gradient become less relevant—this includes the gyro-Bohm mass dependence. Although, TGLF is one of the best models currently available for such simulations and has been steadily improved over the last years, it does not perform similarly well under all conditions [32, 33]. Therefore, we chose to minimize the dependence on the model accuracy by minimizing the effect of the boundary condition. This is done by experimentally matching the pedestal or boundary condition when comparing simulations with different  $M$ . As input to the modelling we use the experimental rotation profile and the fast-ion density, neutral beam particle source and



**Figure 1.** Total pressure at the edge for H and D plasmas with different shaping and different gas puffing. Low gas puffing  $\Gamma \sim 0.9 \times 10^{22} \text{ s}^{-1}$  (a) (H: JPN97095, D: JPN97036) and medium (D: JPN97035) to high (H: JPN97094) gas puffing  $\Gamma \sim 13\text{--}18 \times 10^{22} \text{ s}^{-1}$ .



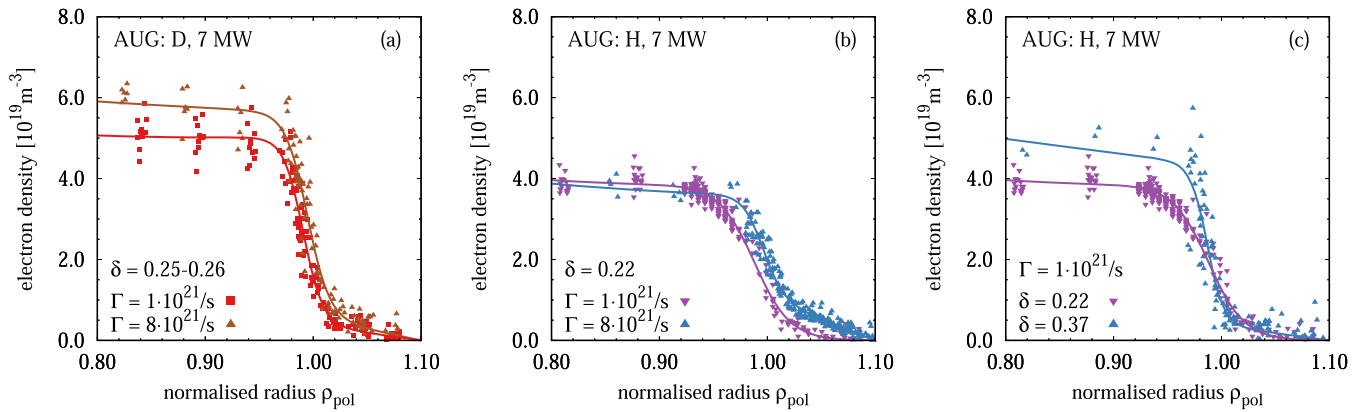
**Figure 2.** Total pressure at the edge for H and D plasmas with different shaping and different gas puffing. Low gas puffing  $\Gamma \sim 0.1 \times 10^{22} \text{ s}^{-1}$  (a) (H: AUG35230, D: AUG35852) and high (H: AUG34716, AUG35231, D: AUG35852) gas puffing  $\Gamma \sim 7\text{--}8 \times 10^{22} \text{ s}^{-1}$ .

heat flux profiles from PENCIL [34] and PION [35] for JET-ILW and from TRANSP [36] for AUG and an experimental boundary condition at  $\rho_{\text{tor}} = 0.85$  for  $T_e$ ,  $T_i$  and  $n_e$ . The fast ions are treated as a non-resonant species in the simulations [37] and no additional effects like non-linear stabilisation of ITGs [38] are taken into account. The temperatures  $T_e$  and  $T_i$  as well as the density  $n_e$  are simulated for  $\rho_{\text{tor}} < 0.85$ .

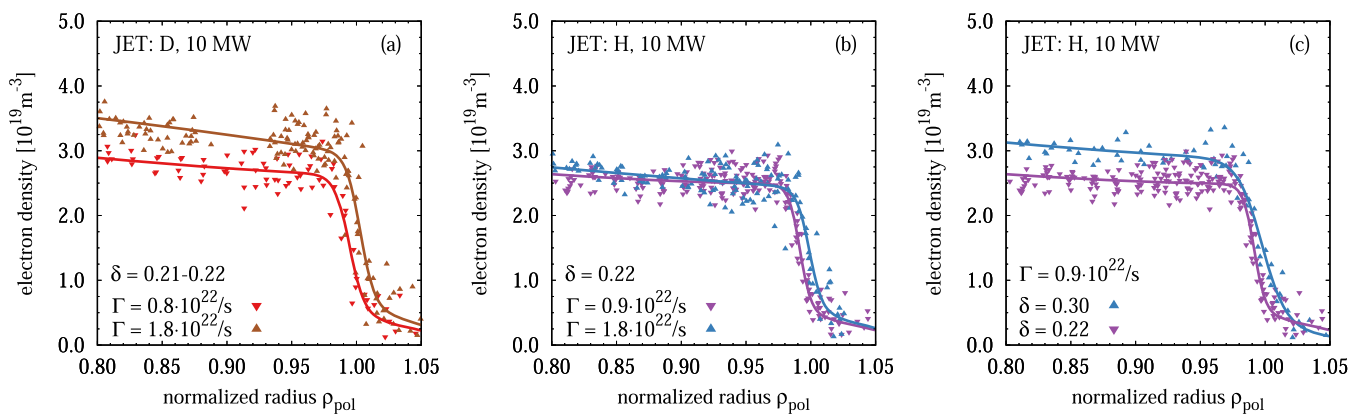
The experimental profiles are obtained with the Fusion-Fit library and all profiles are ELM synchronised and determined in an 2–3 ms time window 1 ms prior to an ELM crash. The main diagnostics are Thomson scattering for  $T_e$  and  $n_e$  [39, 40] and charge exchange  $T_i$  and  $\omega$  [41, 42]. The mapping of the real space to flux space coordinates can be a considerable source of uncertainty. For JET-ILW we use the pressure constrained equilibrium EFTP which results in a different Shafranov shift and pedestal position compared to unconstrained equilibria. In AUG the variation between different equilibrium reconstructions is smaller, but for both machines the profiles are aligned manually to match a separatrix temperature of  $T_e \sim 100 \text{ eV}$ .

### 3. Edge pedestal

As discussed in section 1 we expect a strong mass dependence in the pedestal. This is confirmed by the AUG and JET-ILW data sets discussed in this section. Additionally, we provide evidence to narrow down the potential physics explanations. In figure 1 the thermal plasma pressure is plotted at the plasma edge for different triangularity  $\delta$  and gas puffing  $\Gamma$  in JET-ILW. For low gas puffing shown in figure 1(a) as well as medium to high gas puffing (b) one observes a clear correlation of the pedestal top pressure and isotope mass, namely lower pressure in H compared to D at low  $\delta$ . The variation in  $\delta$  results in a strong impact on the pedestal with increasing pedestal pressure with higher  $\delta$ . The impact of  $\delta$  is stronger in H compared to D in particular for high  $\Gamma$ . This is observed for JET-ILW as shown in figure 1 and for AUG as shown in figure 2 and highlights how  $\delta$  variations can be utilized to match the pedestal between H and D for similar heat sources. This is the first time a matched H-mode pedestal could be obtained in plasmas with different main ion mass while keeping the heating and gas fuelling the same.



**Figure 3.** Electron density profiles for different gas puffing in D (AUG35852) (a) and in H (AUG34716, AUG35230) (b) as well as different  $\delta$  at low gas puffing in H (AUG35230) (c) [5].



**Figure 4.** Electron density profiles for different gas puffing in D (JPN87344, JPN97036) (a) and in H (JPN97094, JPN97095) (b) as well as different  $\delta$  at low gas puffing in H (JPN97095) (c).

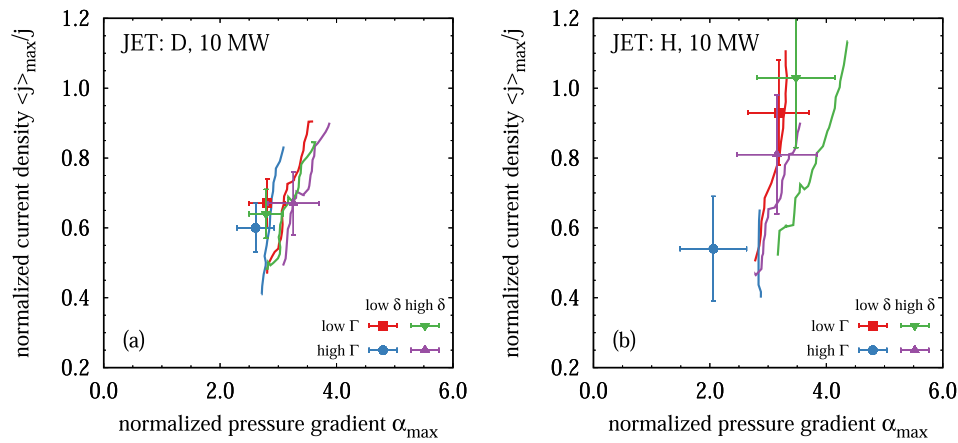
The density pedestal is key in understanding the impact of  $M$  and  $\delta$  on the pedestal and the phenomenology of the density pedestal is remarkably similar in AUG and JET-ILW. This is evident when comparing the profiles shown in figures 3 and 4. In (a) the density increases with increasing gas puff  $\Gamma$  in the D plasmas due to increasing density at the separatrix. This is expected when the ELM behaviour does not change significantly. The same increase in  $\Gamma$  applied to an H plasma does not increase the pedestal top density shown in (b). Simultaneously the total pedestal pressure is reduced by 40% (JET-ILW) and 70% (AUG), as was shown in figures 1 and 2, which for constant density has to be due to a lower temperature. However, when changing  $\delta$  the density can be increased in H up to a level where it matches the D pedestal density at the same gas fuelling without degrading the pedestal temperature as shown in figures 1 and 2(a) and (c). In AUG changing  $\delta$  and  $\Gamma$  has a strong impact on the inter ELM density fluctuation amplitude, measured in the pedestal region with Doppler reflectometry, with high  $\delta$  showing lower fluctuation levels [5]. While being no proof this is a strong indication that the particle transport changes with  $\delta$  and  $\Gamma$ .

As discussed in section 1, the most obvious candidate to understand the pedestal is the ELM stability. The review of

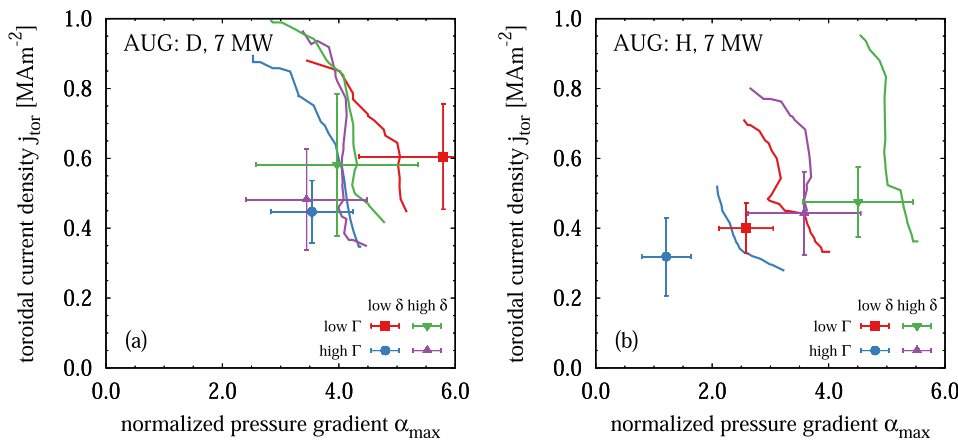
the density profiles indicates that the shifted position of the density profile might contribute to the lower pedestal pressure in H. To test this hypothesis the pedestal stability against peeling–ballooning modes is studied using ELITE [43] (JET-ILW) and MISHKA [44] (AUG) with a HELENA equilibrium [45], the results are shown in figure 5 for the JET-ILW plasmas and figure 6 for the AUG plasmas.

The stability boundary where the growth rate  $\gamma = 0.03$  is indicated as a line. For values of  $\langle j \rangle_{\max} / j$ ,  $\alpha_{\max}$  lower than the boundary the pedestal is considered stable against peeling–ballooning modes. For D we find the stability boundaries for all cases fairly close to each other with the high  $\delta$  cases tending towards higher  $\alpha_{\max}$  as expected. The stability boundaries for the JET-ILW plasmas shown in figure 5 are found around  $\alpha_{\max} \sim 3$  for H and D alike. This suggests that from ideal peeling–ballooning modes no contribution to the observed difference with isotope mass is expected.

When comparing the operational points with their respective stability boundary we find that most JET-ILW plasmas are near the stability boundary. Only the high gas puff  $\Gamma$  and low  $\delta$  H case is found with 30% lower  $\alpha_{\max}$  which also deviates from the peeling–ballooning stability boundary. Figure 6 illustrates the ELM stability for AUG where D plasmas are close to



**Figure 5.** Diagrams of the normalized edge current density  $\langle j \rangle_{\max} / j_{\max}$  and normalized pressure gradient  $\alpha_{\max}$  with the peeling–ballooning stability boundary and the operational point from experiment for a triangularity  $\delta$  and gas puff  $\Gamma$  scan with main ion mass D (a) and H (b) in JET-ILW.



**Figure 6.** Diagrams of the toroidal current density  $j_{\text{tor}}$  and normalized pressure gradient  $\alpha_{\max}$  with the peeling–ballooning stability boundary and the operational point from experiment for a triangularity  $\delta$  and gas puff  $\Gamma$  scan with main ion mass D (a) and H (b) in AUG. [5].

the peeling–ballooning boundary while low  $\delta$  H plasmas are stable against peeling–ballooning modes, in particular, with increasing gas fuelling.

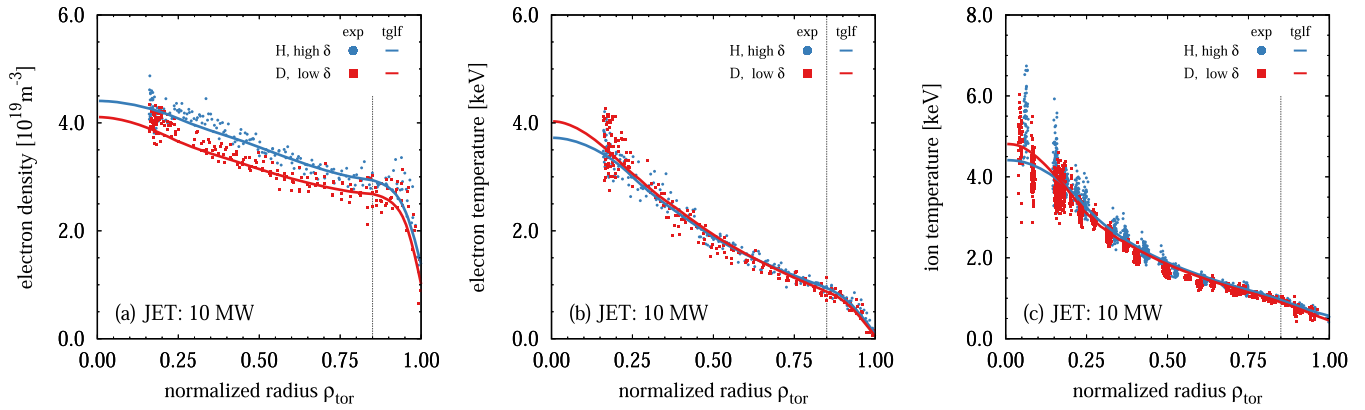
It appears ELM stability cannot explain the observations in low  $\delta$  H plasmas and a mechanism is required to prevent the pedestal from reaching the peeling–ballooning stability limit. High inter-ELM transport could potentially serve this function. The AUG plasma found to be most stable against peeling–ballooning modes is the one with high density fluctuations in the pedestal as discussed above. This is an independent measurement that is consistent with the hypothesis that in AUG the inter ELM transport is important and that its properties change with isotope mass and plasma shape. Comparable measurements of the density fluctuations are not yet available for JET-ILW, still the similar phenomenology of profiles and ELM stability suggests that the same physics mechanisms dominate the plasmas in both machines.

Despite the observed differences in ELM stability, in all the plasmas ELMs are present. It is not trivial to identify the ELM type when the pedestal is deep in the peeling–ballooning stable region. The theoretical framework regarding these type

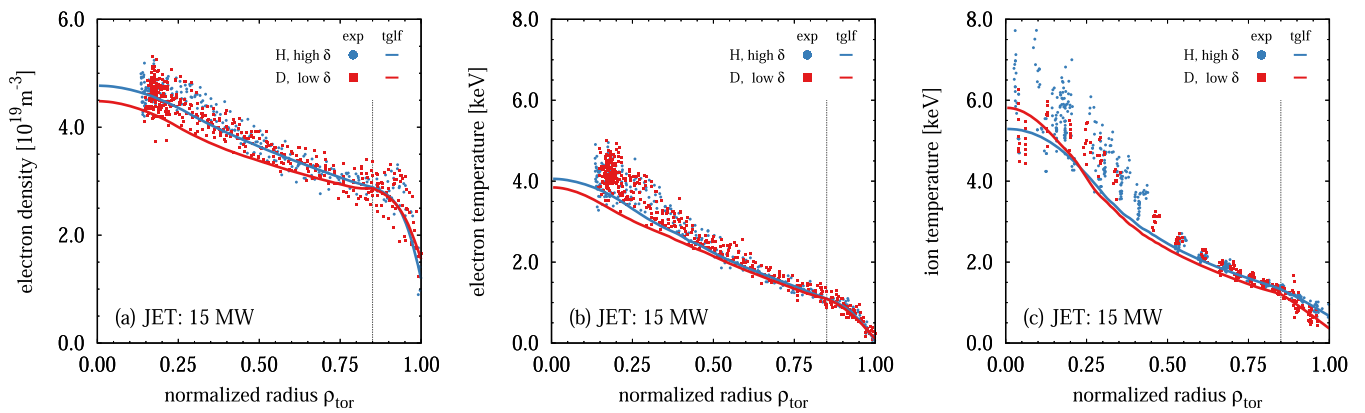
of ELMs is far less developed than that for the ideal peeling–ballooning limited type-I ELMs. Although, new resistive models are being tested against experimental observations which could provide a potential explanation for this type of instability [11], the nature of these ELMs remains an open question.

#### 4. Core transport

As discussed in section 1 we expect different physics mechanisms to contribute to the core transport. In order to quantify the different contributions we compare the experimental results with the quasilinear TGLF transport model using the saturation rule Sat1geo. To minimize the uncertainties due to the treatment of the edge boundary condition in the transport model, we compare plasmas with different main ion mass and different  $\delta$ , but similar pedestal conditions and matched heating and gas puffing. This is the first study of this kind in JET-ILW and allows to analyse the different contributions to the core transport with unprecedented precision.



**Figure 7.** Comparison of a H plasma (JPN97095) and a D plasma (JPN97036) in electron density (a), electron temperature (b) and ion temperature (c). The heating power and gas puff is matched in both cases, while the triangularity is different. The lines correspond to Astra TGLF Sat1geo simulations with the boundary at  $\rho_{\text{tor}} = 0.85$  as indicated by the vertical black dashed line.



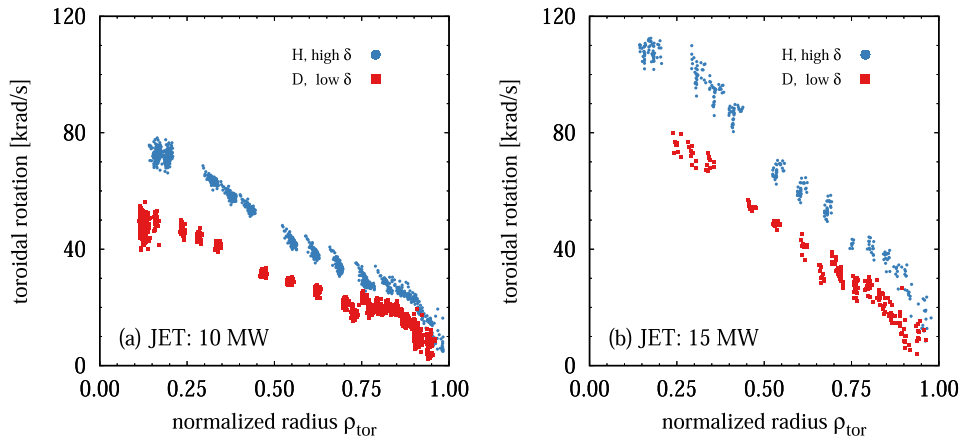
**Figure 8.** Comparison of a H plasma (JPN97096) and a D plasma (JPN96831) in electron density (a), electron temperature (b) and ion temperature (c). The heating power and gas puff is matched in both cases, while the triangularity is different. The lines correspond to Astra TGLF Sat1geo simulations with the boundary at  $\rho_{\text{tor}} = 0.85$  as indicated by the vertical black dashed line.

In figure 7 the profiles for a pair of 10 MW JET-ILW discharges with moderate  $\beta_N = 1.7$  are shown and in figure 8 the same is done for profiles of discharges with 15 MW at higher  $\beta_N \geq 2.5$ . Note this is the first high  $\beta$  H plasma which was achieved in JET. In all four plasmas the only auxiliary heating source is D-NBI. The solid lines in these figures are predictions from the Astra/TGLF simulations with the boundary at  $\rho_{\text{tor}} = 0.85$ . For the moderate  $\beta_N = 1.7$  case shown in figure 7, TGLF predicts the profiles exceptionally well and even reproduces details like the different density peaking between H and D as well the higher core temperature peaking in the ions compared to the electrons. We expect the differences in the density peaking to be transport related, because, the particle source profiles from PION are well matched over most of the radius and only deviate in the very center of the plasma  $\rho_{\text{tor}} < 0.2$  where the volume becomes small. At higher  $\beta_N \geq 2.5$ , TGLF predicts too high transport for H and D, but the general features of the experiment are reproduced, like the differences in core temperature peaking between electrons and ions and more relevant the predicted profiles are practically the same for H and D.

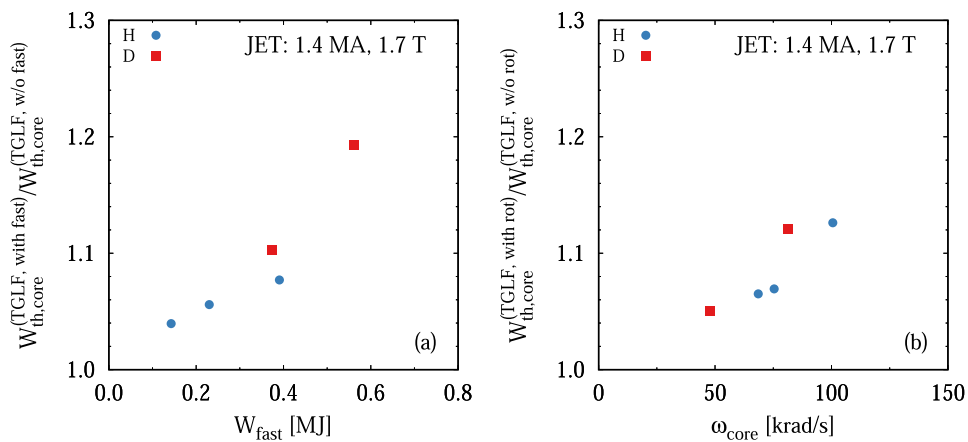
With such a good match between theory and experiment our confidence increases that the model captures the core physics well and we can extract the different contributions to the heat transport from the simulations. This is important because despite the match in the pedestal density and temperatures there are differences between these plasmas besides the main ion mass number. Most notably are the toroidal rotation shown in figure 9 and the fast-ion content. Due to similar torque input by D-NBI, the H plasma with lower inertia rotates faster than the D plasma. While D-NBI also increases the fast-ion content compared to H-NBI, the mass dependence in the slowing down results in lower total fast-ion content in H compared to D. However, with D-NBI the difference in fast-ion content between H and D is lower than if the H plasma is heated with H-NBI.

To test the contribution of main ion mass, rotation and fast-ion content to the core transport we chose the four cases with matched pedestal and an additional H plasma with 10 MW of auxiliary heating with H-NBI. For these five plasmas two additional Astra/TGLF simulations were performed each—one without fast ions  $n_{\text{fast}} = 0$  and one without rotation  $\omega = 0$ .

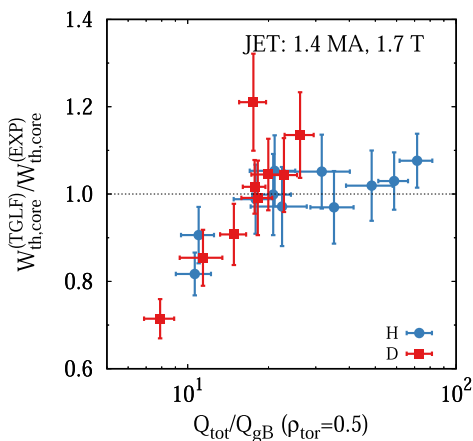




**Figure 9.** Impurity ion rotation profiles for the H–D comparison with matched pedestal pressure using D-NBI and different triangularity for the 10 MW cases (a) and 15 MW cases (b).



**Figure 10.** Change of Astra TGLF Sat1 geo prediction for core contribution to thermal energy when removing fast ions (a) or setting the rotation to zero (b).

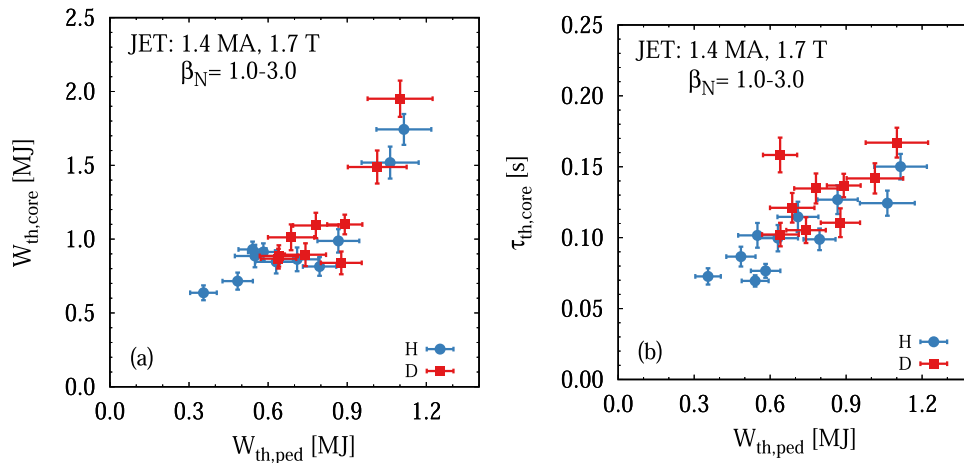


**Figure 11.** Quality of the TGLF prediction in relation to the experiment as a function of heat flux in gyroBohm units at mid-radius for the JET-ILW data set.

In order to systematically compare the simulations we track the changes of the thermal core energy  $W_{\text{th,core}}^{\text{TGLF}}$  resulting from the predicted profiles. We define  $W_{\text{th,core}} = W_{\text{th}} - W_{\text{th,ped}}$  where the pedestal thermal energy  $W_{\text{th,ped}} = 1.5 \int p_{\text{ped}}(\rho_{\text{tor}}) dV$

with  $p_{\text{ped}}(\rho_{\text{tor}}) = \min(p_{\text{ped}}(\rho_{\text{tor}}), p_{\text{ped}}(\rho_{\text{tor}}^{\text{bdry}}))$  and  $\rho_{\text{tor}}^{\text{bdry}} = 0.85$  being the position of the simulation boundary.

The results of this scan are shown in figure 10 where a correlation is observed between the Astra/TGLF prediction and the fast-ion content  $W_{\text{fast}}$  (a) as well as the toroidal rotation in the plasma center  $\omega_{\text{core}}$  (b). In the model both higher fast-ion content and higher rotation yield improved confinement, this improvement is found to be between 5%–10%. Doubling the rotation or fast-ion content has a similar impact on the transport. However the range of fast-ion content accessible in these plasmas is broader than for the rotation. The two contribution go in opposite direction when varying the mass, because typically  $\omega^{\text{H}} > \omega^{\text{D}}$  while  $W_{\text{fast}}^{\text{H}} < W_{\text{fast}}^{\text{D}}$ , therefore, they compensate each other to some extent. The impact of the fast-ion content and the rotation have on the transport in these flux driven simulations also suggests that we are not too close to the critical gradient. In such a situation it would be difficult to extract the mass dependence of the model as discussed in section 2. When simulating the hydrogen discharges with deuterium mass, while keeping all other inputs—heat distribution, fast-ion content, rotation, shape and boundary condition—fixed, the cases with  $M = 2$  are found to have the same core confinement within



**Figure 12.** Core contribution to the thermal plasma energy  $W_{th,core}$  (a) and thermal confinement time  $\tau_{th,core}$  (b) as a function of the edge contribution  $W_{th,ped}$  for different isotope masses in an JET-ILW power/gas scan.

3% both for 10 MW and for 15 MW. This corresponds to a mass scaling of  $W_{th,core} \propto M^{0.00\dots-0.04}$ . The non-existent mass dependence in the core is consistent with the experimental observations, however, this is only seen directly because of the usage of D-NBI in H plasmas. D-NBI compared to H-NBI increases the fast-ion content as well as the rotation. In our data set this reduced the contribution introduced by both parameters when comparing H and D plasmas and allows a more reliable quantification of the mass dependence. When having three parameters—mass, rotation and fast-ions—change in the experiment, it is important to quantify each one or potentially the impact of one might be confused with the other.

To assess the quality of the TGLF predictions of the core transport, the whole set of simulations is compared with the experimental profiles. This includes the matched plasmas described above and additionally those with high  $\delta$  in D and low  $\delta$  in H and consequently different pedestal top pressures. In figure 11 the deviation ratio between the experiment and the prediction is plotted as a function of the heat fluxes at mid-radius in gyroBohm units  $Q_{tot}/Q_{gB}$ . One finds that TGLF predicts the core confinement accurately within  $\pm 5\%$  for  $Q_{tot}/Q_{gB} > 17$ . In particular, for H this is true despite a variation of the pedestal pressure by over a factor of 2 (cp to figure 1).

From the points which exhibit a larger deviation between model and experiment important information can be deduced. First there is a single plasma in the data set with a neoclassical tearing mode with mode numbers  $(m, n) = (3, 2)$ . For a plasma with core MHD activity the model should overestimate the confinement, because, the magnetic island is not treated in the model. In figure 11 this plasma at  $Q_{tot}/Q_{gB} = 17$  is clearly visible as outlier with  $W_{th,core}^{(TGLF)}/W_{th,core}^{(EXP)} = 1.15$  as is expected. This highlights that we can identify changes in the core transport with the chosen representation which increases our confidence in the validity of our interpretation.

For  $Q_{tot}/Q_{gB} < 17$  TGLF starts to overestimate the core transport in H and D plasmas leading to lower  $W_{th,core}$ . Since for the first time in JET-ILW a heating power of 15 MW was introduced in a H plasma with good pedestal performance we

were able to populate the  $Q_{tot}/Q_{gB} < 17$  region with H data points. This gives crucial new insight for the interpretation of the data. As a thought experiment, we discuss the data set as if these two new H points were not present. Then a clear separation between H and D plasmas would remain. This might be interpreted such that theory overestimates the core heat transport in deuterium plasmas and a yet unknown isotope effect is necessary to bridge the gap between H and D plasmas. However, the separation in gyro-Bohm units is not only due to the mass dependence in the normalisation, but also due to the mass dependence in the pedestal temperature and density as described in section 3. A lower pedestal top will result in larger heat fluxes in gyro-Bohm units, despite the same experimental heat fluxes. I.e. the isotope dependence of the pedestal can have a significant impact on the interpretation of core transport modelling.

However, the new H plasmas, with high heating and high  $\delta$ , show the same overestimated core heat transport in the modelling as do the D plasmas. This suggests that the shortcoming of the model for  $Q_{tot}/Q_{gB} < 17$  does not originate in the isotope mass and is instead connected to an accurate prediction of threshold and stiffness properties of heat transport under these conditions.

This overestimation of the core transport in H and D plasmas at low  $Q_{tot}/Q_{gB}$  by TGLF was also observed in comparisons with non-linear gyrokinetic Gene simulations [33]. For such plasmas with higher  $\beta_e$  the nonlinear electromagnetic turbulence stabilisation—which is not present in TGLF—becomes more important [32, 46, 47]. Non-linear stabilisation of ITGs via fast ions [21, 38, 48] is likely not responsible for this difference. In the AUG core transport an empirical threshold of  $W_{fast}/W_{th} > 1/3$  was found for NBI heated plasmas [4]. The JET-ILW 1.4 MA, 1.7 T, H and D plasmas all have  $W_{fast}/W_{th} < 1/4$ . In order to contribute to this questions non-linear gyrokinetic simulations will be performed for our data set in the near future.

To approach this open question from the experimental side in figure 12(a) the core–edge coupling of the plasma energy between H and D is shown. While a correlation

between  $W_{\text{th,core}}$  and  $W_{\text{th,ped}}$  is not entirely surprising as it was observed before, for example, in JET-ILW [19]. In our data set the heating power is varied by over a factor of 2 and the pedestal top is varied via the shaping at constant heating power and still the correlation between edge and core holds. Further, in figure 12(b) it is shown that the core confinement time  $\tau_{\text{th,core}} = W_{\text{th,core}}/P_{\text{sep}}$ , with  $P_{\text{sep}} = P_{\text{heat}} - P_{\text{rad}}$ , even increases with increasing pedestal top. This is not trivial as one would expect a strong power degradation with increasing  $P_{\text{sep}}$  which is still visible in the two outliers towards higher  $\tau_{\text{th,core}}$  at  $W_{\text{th,ped}} = 0.7$  MJ which are the D plasmas with the lowest heating power. However, since the data set is not only a power scan and  $W_{\text{th,ped}}$  is varied via  $M$ ,  $\Gamma$  and  $\delta$  as well, it makes sense to consider additional mechanisms. When one excludes fast ion effects a remaining candidate is  $\beta$  stabilisation where the experimental reasoning is that  $\beta$  is one of the few core parameters which is directly affected by the pedestal. However, a higher pedestal also reduces  $R/L_T \propto 1/T$  and thereby the turbulence drive. In simple transport simulations with a coupled edge-core model a doubling of the pedestal pressure at constant input power results in 50% higher  $W_{\text{th,core}}$  for the same core transport model. This is the same magnitude as observed in the experiment.

Independently of the potential explanations the data shows no significant deviation between H and D plasmas. But since H plasmas are on average found with a lower pedestal energy  $W_{\text{th,ped}}$  than their D counterparts, also the core confinement time will be lower in H on average. Given our observations we conclude that the improvement of core confinement is not a consequence of an isotope mass dependence in the core transport, but a consequence of the core–edge coupling which is found in H and D plasmas alike.

## 5. Summary

While performing experiments with different main ion masses, the mass number is never the only parameter that is changing. We rather observe different overlapping effects. Most notably is the core–edge coupling. Changes in the edge will impact the core and vice versa. In the pedestal a very strong dependence on the mass number and the gas fuelling is observed. This will have direct consequences for the core confinement time— independent of the main ion mass.

Where the parameter space in AUG and JET-ILW overlaps, plasmas exhibit the same physics responses to changes in the engineering parameters. This is found for the core transport at moderately low fast-ion content and for the strong isotope mass dependence of the pedestal, which is comparable in both machines. At the edge the inter-ELM transport is the most promising candidate to explain the experimental observations. However, the detailed underlying physics mechanisms could not be identified due to the lack of accurate transport modelling of the steep gradient region in the H-mode edge.

When the edge isotope dependence is offset by varying the triangularity at the separatrix Astra/TGLF (Sat1geo) simulations predict the core transport surprisingly well for moderate  $\beta$ . In the simulations of the core transport, fast-ion and rotation effects are small but larger than the isotope mass dependence






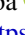


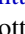



which is close to nonexistent. This is different in AUG when the fast-ion content between H and D diverges at higher NBI power density and non-linear turbulence stabilisation due to fast ions starts playing a role [4]. This is consistent with JET-ILW where the relative fast-ion content is lower than in AUG and the effect of thermal ion dilution by fast ions is sufficient to model the observations.

For the first time an isotope study between H and D could be extended to high  $\beta$  H plasmas. This is only possible due to the pedestal match with different  $\delta$  and an increase of the heating power in H by applying D-NBI. This allows to investigate the isotope dependence of the EM stabilisation. While the experimental data suggests only a small impact of the main ion mass on the core transport also for high  $\beta$  plasmas, a detailed comparison to advanced theoretical models is still missing and will be subject to future investigations.

## Acknowledgments

This work has been carried out within the framework of the EUROfusion Consortium and has received funding from the Euratom research and training programme 2014–2018 and 2019–2020 under Grant Agreement No. 633 053. The views and opinions expressed herein do not necessarily reflect those of the European Commission.

## ORCID iDs

P.A. Schneider  <https://orcid.org/0000-0001-7257-3412>  
 C. Angioni  <https://orcid.org/0000-0003-0270-9630>  
 L. Frassinetti  <https://orcid.org/0000-0002-9546-4494>  
 L. Horvath  <https://orcid.org/0000-0002-5692-6772>  
 F. Auriemma  <https://orcid.org/0000-0002-1043-1563>  
 J.M. Fontdecaba  <https://orcid.org/0000-0001-7678-0240>  
 J. Hobirk  <https://orcid.org/0000-0001-6605-0068>  
 A. Kappatou  <https://orcid.org/0000-0003-3341-1909>  
 C.F. Maggi  <https://orcid.org/0000-0001-7208-2613>  
 R.M. McDermott  <https://orcid.org/0000-0002-8958-8714>  
 T. Pütterich  <https://orcid.org/0000-0002-8487-4973>  
 M. Willensdorfer  <https://orcid.org/0000-0002-1080-4200>

## References

- [1] ITER Physics Basis Expert Groups on Confinement and Transport and Confinement Modelling and Database, ITER Physics Basis Editors 1999 *Nucl. Fusion* **39** 2175
- [2] Cordey J 1999 *Nucl. Fusion* **39** 1763
- [3] Laggner F.M. *et al* 2017 *Phys. Plasmas* **24** 56105
- [4] Schneider P.A. *et al* 2021 *Nucl. Fusion* **61** 036033
- [5] Schneider P.A. *et al* 2021 *Plasma Phys. Control. Fusion* **63** 64006
- [6] Maggi C.F. *et al* 2018 *Plasma Phys. Control. Fusion* **60** 14045
- [7] Horvath L. *et al* 2021 *Nucl. Fusion* **61** 046015
- [8] Huysmans G.T.A., Sharapov S.E., Mikhailovskii A.B. and Kerner W. 2001 *Phys. Plasmas* **8** 4292
- [9] Aiba N. *et al* 2017 *Nucl. Fusion* **57** 126001
- [10] Dunne M.G. *et al* 2017 *Plasma Phys. Control. Fusion* **59** 14017
- [11] Frassinetti L. *et al* 2021 *Nucl. Fusion* **61** 126054

- [12] Schneider P.A. *et al* 2015 *Plasma Phys. Control. Fusion* **57** 14029
- [13] Bonanomi N., Angioni C., Crandall P.C., Di Siena A., Maggi C.F. and Schneider P.A. 2019 *Nucl. Fusion* **59** 126025
- [14] Belli E.A., Candy J. and Waltz R.E. 2020 *Phys. Rev. Lett.* **125** 15001
- [15] Viezzer E. *et al* 2018 *Nucl. Fusion* **58** 026031
- [16] Nakata M. *et al* 2017 *Phys. Rev. Lett.* **118** 165002
- [17] Bustos A., Bañón Navarro A., Görler T., Jenko F. and Hidalgo C. 2015 *Phys. Plasmas* **22** 012305
- [18] Garcia J. *et al* 2018 *Phys. Plasmas* **25** 55902
- [19] Weisen H. *et al* 2020 *J. Plasma Phys.* **86** 905860501
- [20] Schneider P.A. *et al* 2017 *Nucl. Fusion* **57** 066003
- [21] Bonanomi N. *et al* 2019 *Nucl. Fusion* **59** 096030
- [22] Challis C.D. *et al* 2015 *Nucl. Fusion* **55** 053031
- [23] Garcia J., Challis C., Citrin J., Doerk H., Giruzzi G., Görler T., Jenko F. and Maget P. 2015 *Nucl. Fusion* **55** 053007
- [24] Härtl T., Rohde V. and Mertens V. 2015 *Fusion Eng. Des.* **96–97** 265
- [25] Carvalho I.S. *et al* 2017 *Fusion Eng. Des.* **124** 841
- [26] Chankin A.V. *et al* 2019 *Plasma Phys. Control. Fusion* **61** 75010
- [27] Camenen Y., Pochelon A., Behn R., Bottino A., Bortolon A., Coda S., Karpushov A., Sauter O. and Zhuang G. (the TCV team) 2007 *Nucl. Fusion* **47** 510
- [28] Dunne M.G. *et al* 2017 *Plasma Phys. Control. Fusion* **59** 25010
- [29] Staebler G.M., Howard N.T., Candy J. and Holland C. 2017 *Nucl. Fusion* **57** 066046
- [30] Pereverzev G.V. *et al* 2002 *IPP Report 5/98* (<http://hdl.handle.net/11858/00-001M-0000-0027-4510-D>)
- [31] Fable E. *et al* 2013 *Plasma Phys. Control. Fusion* **55** 124028
- [32] Reisner M., Fable E., Stober J., Bock A., Bañón Navarro A., Di Siena A., Fischer R., Bobkov V. and McDermott R. 2020 *Nucl. Fusion* **60** 082005
- [33] Mariani A., Mantica P., Casiraghi I., Citrin J., Görler T. and Staebler G.M. (EUROfusion JET1 contributors) 2021 *Nucl. Fusion* **61** 066032
- [34] Challis C.D., Cordey J.G., Hamnén H., Stubberfield P.M., Christiansen J.P., Lazzaro E., Muir D.G., Stork D. and Thompson E. 1989 *Nucl. Fusion* **29** 563
- [35] Eriksson L.-G., Hellsten T. and Willen U. 1993 *Nucl. Fusion* **33** 1037
- [36] Breslau J. *et al* 2018 *TRANSP, [Computer Software]* (<https://doi.org/10.11578/dc.20180627.4>)
- [37] Tardini G. *et al* 2007 *Nucl. Fusion* **47** 280
- [38] Citrin J. *et al* 2013 *Phys. Rev. Lett.* **111** 155001
- [39] Kurzan B. and Murmann H.D. 2011 *Rev. Sci. Instrum.* **82** 103501
- [40] Frassinetti L. *et al* 2012 *Rev. Sci. Instrum.* **83** 13506
- [41] McDermott R.M. *et al* 2017 *Rev. Sci. Instrum.* **88** 73508
- [42] Hawkes N.C., Delabie E., Menmuir S., Giroud C., Meigs A.G., Conway N.J., Biewer T.M. and Hillis D.L. 2018 *Rev. Sci. Instrum.* **89** 10D113
- [43] Wilson H.R., Snyder P.B., Huysmans G.T.A. and Miller R.L. 2002 *Phys. Plasmas* **9** 1277
- [44] Mikhailovskii A.B. *et al* 1997 *Plasma Phys. Rep.* **23** 844
- [45] Huysmans G.T.A., Goedbloed J.P. and Kerner W. 1991 *Int. J. Mod. Phys. C* **02** 371
- [46] Citrin J. *et al* 2014 *Nucl. Fusion* **54** 023008
- [47] Doerk H., Challis C., Citrin J., Garcia J., Görler T. and Jenko F. 2016 *Plasma Phys. Control. Fusion* **58** 115005
- [48] Di Siena A. *et al* 2018 *Phys. Plasmas* **25** 42304